Talanta 231 (2021) 122367

Contents lists available at ScienceDirect

Talanta

journal homepage: www.elsevier.com/locate/talanta

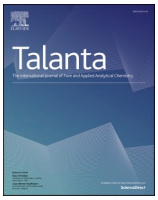

Intra-laboratory comparison of four analytical platforms for lipidomic quantitation using hydrophilic interaction liquid chromatography or supercritical fluid chromatography coupled to quadrupole - time-of-flight mass spectrometry

Michaela Chocholoušková [a], Denise Wolrab [a], Robert Jirásko [a], Hana Študentová [b], Bohuslav Melichar [b], Michal Holčapek [a,*]

[a] University of Pardubice, Faculty of Chemical Technology, Department of Analytical Chemistry, Studentská 573, 532 10, Pardubice, Czech Republic
[b] Palacký University, Medical School and Teaching Hospital, Department of Oncology, I.P. Pavlova 6, 775 20, Olomouc, Czech Republic

ARTICLE INFO

Keywords:
Hydrophilic interaction liquid chromatography
Supercritical fluid chromatography
Mass spectrometry
Lipidomics
Quantitation
Plasma
Normalization

ABSTRACT

The lipidomic research is currently devoting considerable effort to the harmonization that should enable the generation of comparable and accurate quantitative lipidomic data across different laboratories and regardless of the mass spectrometry-based platform used. In the present study, we systematically investigate the effects of the experimental setup on quantitative lipidomics data obtained by two lipid class separation approaches, hydrophilic interaction liquid chromatography (HILIC) and ultrahigh-performance supercritical fluid chromatography (UHPSFC), coupled to two different quadrupole – time of flight (QTOF) mass spectrometers from the same vendor. This approach is applied for measurements of 268 human plasma samples of healthy volunteers and renal cell carcinoma patients resulting in four data sets. We investigate and visualize differences among these data sets by multivariate data analysis methods, such as principal component analysis (PCA), orthogonal partial least square discriminant analysis (OPLS-DA), box plots, and logarithmic correlations of molar concentrations of individual lipid species. The results indicate that even measurements in the same laboratory for the same samples using different analytical platforms may yield slight variations in the molar concentrations determined. The normalization to a reference sample with defined lipid concentrations can further diminish these small differences, resulting in highly homogenous molar concentrations of individual lipid species. This strategy indicates a potential approach towards the reporting of comparable quantitative results independent from the quantitative approach and mass spectrometer used, which is important for a wider acceptance of lipidomics data in various biomarker inter-laboratory studies and ring trials.

1. Introduction

Lipidomics is a quickly developing research field focused on the investigation of lipids in biological systems including the structural analysis, determination of functions, and interactions with other metabolites and proteins [1]. Lipidomics is frequently involved in clinical studies, because of the importance of lipids in human body and the role in cellular biology, metabolic processes, and the pathological conditions including cancer, cardiovascular disorders, diabetes mellitus, obesity, and infectious diseases [2–7].

In pathophysiological considerations, lipids are usually not considered as single molecular species, but rather as a group of molecules. Therefore, the fundamental requirement to understand the role of lipids at the cellular, tissue, and whole body levels is a comprehensive and quantitative analysis [2,8]. Chromatography coupled to mass spectrometry (MS) belongs to key approaches used for the identification and quantitation of lipids in biological samples due to a relatively wide range of separation principles useful for the separation of different types of lipid isomers. Based on the chromatographic mode, it is possible to achieve either lipid class or lipid species separation [6,9–12]. Both strategies have limitations and advantages, mainly associated with the selection and number of internal standards (IS) spiked into samples

* Corresponding author.
E-mail address: Michal.Holcapek@upce.cz (M. Holčapek).

https://doi.org/10.1016/j.talanta.2021.122367
Received 18 January 2021; Received in revised form 21 March 2021; Accepted 22 March 2021
Available online 2 April 2021

before the extraction, which is necessary for the optimal quantitation performance [9,13]. Lipid class separation requires at least one IS per lipid class, because of the coelution of IS and endogenous lipids, which guarantees the same matrix effects and the ion suppression necessary for the accurate quantitation. In lipidomic analysis, prerequisite of the best quantitation practice is the use of appropriate IS with the concentrations close to the physiological values. The common approach for a selection of IS is the use of exogenous lipid species not occurring in studied biological samples, such as lipids with shorter/longer fatty acyl chains, or an odd number of carbon atoms, but the best choice is to use isotopically labeled lipid species (e.g., D or ^{13}C) [11,14]. Outcome information of lipid structure using lipid class separation is the sum of carbon number (CN) and double bonds (DB) without detailed structural information, such as positions of DB or exact fatty acyl bonded to the glycerol backbone (advantage of lipid species separation, such as reversed-phase chromatography) [6,13]. Hydrophilic interaction ultrahigh -performance liquid chromatography (HILIC-UHPLC) or ultrahigh -performance supercritical fluid chromatography (UHPSFC) are two chromatographic approaches leading to the lipid class separation based on interactions between polar head groups of lipids, polar stationary phase, and less polar mobile phase [15,16]. High-resolution mass spectrometers, such as quadrupole time-of-flight (QTOF) mass spectrometer equipped with electrospray ionization (ESI) as the most universal ionization technique [17], belongs to the most common configurations used in the lipidomic analysis [18,19].

A lack of methodological standardization makes the lipidomic research challenging. There are still no guidelines for lipidomic workflows covering the whole process from the extraction to the measurements and data processing with missing harmonization of reporting results, constituting currently a limitation of lipidomics. Furthermore, a great variety of mass spectrometers from various manufacturers are on the market with different geometry, ionization technique, operating conditions, and settings. This diversity along with other issues including various sample extraction protocols, IS used, and instrumental setups may have an impact on the quantitative lipidomic results [2,19,20].

MS-based methods coupled to chromatographic methods represent the principal approaches for lipidomic analysis. The principal aim of this study was an intra-laboratory comparison between four platforms including two quadrupole – time of flight (QTOF) mass spectrometers from the same vendor (**Xevo G2-XS-QTOF** and **Synapt G2-Si-QTOF**) connected to HILIC-UHPLC (Agilent 1290 Infinity series UHPLC system) and UHPSFC systems (Acquity UPC^2 UHPSFC system) using the same samples and extracts. The key scientific question is to evaluate the extent of differences in molar concentrations depending on the mass spectrometer employed and the hyphenated chromatographic technique used for the analysis of plasma samples obtained from a cohort of renal cell carcinoma patients and healthy volunteers.

2. Materials and methods

2.1. Chemicals and solvents

LC/MS grade solutions and additives, including acetonitrile, methanol, 2-propanol, hexane, water, ammonium carbonate, and ammonium acetate (Honeywell, Riedel-de Haën, Germany), were purchased from Thermo Fisher Scientific (Waltham, MA, USA). Chloroform (Lichrosolv) was purchased from Merck (Darmstadt, Germany) and supercritical carbon dioxide ($scCO_2$) with 99.995% purity from Messer (Bad Soden, Germany). Deionized water used for the preparation of mobile phases in HILIC-UHPLC/MS method and for the preparation of ammonium carbonate buffer (for extraction) was obtained from Milli-Q water purification system (Millipore, Molsheim, France). Lipid IS, such as 15:0–18:1-d7 glycerophosphocholine (**PC 33:1 D7**), 14:0–14:0 glycerophosphocholine (**PC 28:0**), 22:0–22:0 glycerophosphocholine (**PC 44:0**), 22:1–22:1 glycerophosphocholine (**PC 44:2**), 18:1-d7 glycerophosphocholine (**LPC 18:1 D7**), 17:0 glycerophosphocholine (**LPC 17:0**), 18:1-d9 sphingomyelin (**SM 36:2 D9**), 12:0 sphingomyelin (**SM 30:1**), 15:0–18:1-d7-15:0 triacylglycerol (**TG 48:1 D7**), 15:0–18:1-d7 diacylglycerol (**DG 33:1 D7**), 18:1–18:1-d5 diacylglycerol (**DG 36:2 D5**), 18:1-d7 monoacylglycerol (**MG 18:1 D7**), 19:1 monoacylglycerol (**MG 19:1**), 16:0 cholesteryl-d7 ester (**CE 16:0 D7**), d18:1-d7/18:0 ceramide (**Cer C18 D7**), d18:1/17:0 ceramide (**Cer 35:1**), and d18:1/12:0 ceramide (**Cer 30:1**), manufactured by Avanti Polar Lipids (Alabaster, AL, USA) were purchased from Merck. IS 19:1–19:1–19:1 triacylglycerol (**TG 57:3**) and 12:1–12:1 diacylglycerol (**DG 24:2**) were purchased from Nu-Chek (Elysian, MN, USA).

2.2. Human plasma samples

Human plasma samples (heparin-lithium) from 95 healthy volunteers (44 females and 51 males), 173 renal cell carcinoma patients (51 females and 122 males) were collected (268 samples in total) at the Medical School and Teaching Hospital in Olomouc based on the approval of institutional ethical committee. All subjects signed an informed consent. For the quality control (QC), a pooled sample of individual plasma samples was prepared. As a standard reference material, SRM 1950 Metabolites in Frozen Human plasma (NIST, Gaithersburg, MD) was used (further abbreviation as NIST plasma).

2.3. Sample preparation

Plasma samples were prepared using a double Folch extraction with some modifications as outlined below. Briefly, 20 μL of a mixture of IS (IS Mix) were added to 25 μL of plasma, followed by the addition of 3 mL chloroform/methanol mixture (2:1, *v/v*), and ultrasonicated for 15 min in a water bath. Subsequently, 600 μL of 250 mM aqueous ammonium carbonate were added to the homogenate, and the mixture was ultrasonicated for 15 min. After the centrifugation (3 min, 1730 g), the organic layer was removed to a new vial, and 2 mL of chloroform were added to the aqueous phase. The mixture was ultrasonicated for 15 min, centrifuged (3 min, 1730 g), and the organic phase was transferred and mixed with the previously collected organic phase. After the evaporation under nitrogen, the residue was reconstituted in 500 μL of chloroform/methanol mixture (1:1, *v/v*). The plasma extract was 5-times diluted using chloroform/methanol mixture (1:1, *v/v*) and injected.

The final concentrations of IS in IS Mix are shown in Table S-1 in Electronic Supplementary Material (ESM), and the preparation of IS Mix was described in our previous paper [21].

2.4. HILIC-UHPLC conditions

An Agilent 1290 Infinity series UHPLC system (Agilent Technologies, Waldbronn, Germany) was used for HILIC-UHPLC experiments with the following conditions: the column Viridis BEH Waters (100 × 3 mm, 1.7 μm), the temperature of separation 40 °C, the flow rate 0.5 mL/min, and the injection volume 1 μL. The injection needle was washed with a mixture of methanol/acetonitrile/2-propanol/water (1:1:1:1, *v/v/v/v*) after each injection. The mobile phase A was acetonitrile/water (96/4, *v/v*), the mobile phase B was acetonitrile/water (2/98, *v/v*), and both phases contained 8 mM of ammonium acetate. The following linear gradient was used: 0–5 min (100–84% of mobile phase A), 5–5.5 min (84% of mobile phase A), and 5.51–10.5 min (100% of mobile phase A). The autosampler temperature was set to 4 °C [21].

2.5. UHPSFC conditions

An Acquity UPC^2 instrument from Waters (Milford, MA, USA) was used for UHPSFC experiments with the following conditions: the column Viridis BEH Waters (100 × 3 mm, 1.7 μm), the column temperature to 60 °C, the flow to 1.9 mL/min, and the injection volume was 1 μL. The injection needle was washed with hexane/2-propanol/water (2:2:1, *v/v/v*) after each injection. The following gradient was employed using

$scCO_2$ and MeOH (30 mM ammonium acetate + 1% of water) as a modifier: 0 min–1% modifier, 1.5 min–16% modifier, 4 min–51% modifier, 7 min–51% modifier, 7.51 min–1% modifier, and the equilibration with the total run time of 8 min. The automatic back-pressure regulator (ABPR) was set to 1800 psi and the autosampler temperature to 4 °C. Methanol with 30 mM ammonium acetate and 1% of water was used as the make-up solvent with a flow rate of 0.25 mL/min [21].

2.6. MS conditions - Xevo G2-XS-QTOF

Xevo G2-XS-QTOF mass spectrometer (Waters, Milford, MA, USA) was used in the sensitivity mode (vendor setting) using the positive ion ESI mode under the following conditions: the capillary voltage of 3 kV, the sampling cone of 20 V, the source offset of 90 V, the source temperature of 150 °C, the desolvation temperature of 500 °C, the cone gas of 50 L/h, and the desolvation gas flow of 1000 L/h. Mass spectra were measured in the *m/z* range of 150–1200 with the scan time of 0.5 s using the continuum mode and the peptide leucine enkephalin as a lock mass.

2.7. MS conditions - Synapt G2-Si-QTOF

Hybrid quadrupole - time of flight (QTOF) mass spectrometer Synapt G2-Si (Waters) was used with the following conditions: the sensitivity mode applying positive ESI mode, the mass range of *m/z* 150–1200, the capillary voltage of 3 kV, the sampling cone of 20 V, the source offset of 90 V, the source temperature of 150 °C, the desolvation temperature of 500 °C, the cone gas flow of 50 L/h, the desolvation gas flow of 1000 L/h, and the nebulizer gas pressure of 4 bar. Mass spectra were acquired in the continuum mode with a scan time of 0.1 s, and the peptide leucine enkephalin was used as the lock mass.

2.8. Data analysis

All HILIC-UHPLC/MS and UHPSFC/MS spectra were acquired using MassLynx. The Compression tool (Waters) was used for the noise reduction and the Accurate mass measure tool (Waters) for the lock mass correction and the conversion from continuum to centroid spectra. MarkerLynx was used to obtain tables of *m/z* features with the corresponding intensities in all samples. Lipid identification and quantitation including isotopic correction were performed using the LipidQuant script in the Microsoft Excel. R 3.6.1 free software environment using readxl and ggplot2 packages (for box plots), Microsoft Excel (for calculations of residual standard deviations (RSD), correlation plots, bar plots, normalization, etc.), and the SIMCA software 13.0.3 (PCA and OPLS-DA plots) (Umetrics AB, Umeå, Sweden) were used for statistical evaluation. Only lipid species with a detectable concentration present in at least 75% cases of all samples were included in the data set. For zero filling, 80% of the minimum concentration value for each lipid species considering all 268 samples were used [21,22].

3. Results and discussion

3.1. Study design

The same chromatographic instruments and identical conditions, including column, chromatography settings, mobile phase composition and additives, were used; for both HILIC-UHPLC and UHPSFC to connect to both mass spectrometers to get the four analytical platforms abbreviated as **HILIC-Xevo**, **HILIC-Synapt**, **UHPSFC-Xevo**, and **UHPSFC-Synapt**. Both mass spectrometers are equipped with the same ion source geometry with the same setting and the same ultra-fast electron multiplier and hybrid ADC detector electronics. Detailed parameters of both mass spectrometers are listed in Table S-2 in ESM. It was not possible to set exactly the same values of some MS parameters for both mass spectrometers, due to the limited access to settings, the instrumental characteristics, and specific service tuning procedures.

All samples (268) were randomized for extractions and for measurements, and the same sequence tables as well as the same extracts were used for the measurements. The sample sequence included blank samples ($CHCl_3$/MeOH (1:1)), QC samples, system standard samples (SSS; neat mixture of lipid standards with 18:1 fatty acyls), and NIST plasma sample as a reference material.

3.2. Chromatography and MS

The total run times of high-throughput HILIC/MS and UHPSFC/MS analyses were 10.5 min and 8 min, respectively. Examples of illustrative chromatograms of NIST plasma for the four analytical platforms are shown in Fig. S-1. In case of HILIC/MS, non-polar lipids, such as triacylglycerols (TG), diacylglycerols (DG), monoacylglycerols (MG), and cholesteryl esters (CE), elute in the void volume and ceramides (Cer) shortly after the void volume. In case of UHPSFC/MS, all classes of non-polar lipids are chromatographically separated, which eliminates the problem with in-source fragmentation of TG that results in a mass overlap of DG and MG fragment ions. This allows the quantitation of DG and MG in contrast to HILIC/MS in which these lipid classes cannot be quantified.

Mass spectra were acquired in the positive-ion mode using ESI in the sensitivity mode (vendor setting). There are several parameters, which can influence the ionization yield and the adduct formation, including the mobile phase composition, additives, flow rate, sample matrix, and ion source settings. The adducts present in mass spectra for individual lipid classes and their ratios demonstrated on deuterated IS in the NIST plasma sample measured at the beginning, in the middle, and at the end of the sequence (mean value) are listed in Table 1. Protonated molecules together with $[M+Na]^+$ adducts are present for phosphatidylcholines (PC), lysophosphatidylcholines (LPC), sphingomyelins (SM), and CE. In case of PC and SM, the protonated molecules show a higher response for all analytical platforms, therefore $[M+H]^+$ ions were used for the quantitation. In case of LPC, the ratio between protonated molecules and sodium adducts depends on the chromatographic mode, where $[M+Na]^+$ adducts have a higher response than protonated molecules for HILIC/MS, while it is opposite for UHPSFC/MS. To compare the four platforms between each other, $[M+H]^+$ ions of LPC were used for the

Table 1
Ions of deuterated IS present in mass spectra of NIST plasma sample at the beginning, middle, and the end of sequence (average value). Ions used for the quantitation are involved.

Internal standard	Ions	HILIC-Xevo %	HILIC-Synapt %	UHPSFC-Xevo %	UHPSFC-Synapt %
TG 48:1 d7	**$[M+NH4]^+$**	100	100	100	100
	$[M+Na]^+$	31.9	33.5	10.2	1.5
Cer36:1 d7	**$[M+H–H_20]^+$**	100	100	100	100
	$[M+Na]^+$	76.9	2.7	25.4	0.7
	$[M+H]^+$	49.7	0.8	23.4	0.7
PC 33:1 d7	**$[M+H]^+$**	100	100	100	100
	$[M+Na]^+$	14.7	7.2	6.4	0.5
LPC 18:1 d7	**$[M+H]^+$**	17.6	16.0	100	100
	$[M+Na]^+$	100	100	4.1	0.7
SM 36:2 d9	**$[M+H]^+$**	100	100	100	100
	$[M+Na]^+$	29.0	18.2	26.9	19.0
DG 33:1 d7	**$[M+H–H_20]^+$**	–	–	100	100
	$[M+Na]^+$	–	–	48.7	27.0
	$[M+NH_4]^+$	–	–	19.5	6.6
MG 18:1 d7	**$[M+Na]^+$**	–	–	100	100
	$[M+H–H20]^+$	–	–	67.2	70.1
	$[M+NH_4]^+$	–	–	5.1	–
CE 16:0 d7	**$[M+Na]^+$**	–	–	100	100
	[M+H]+	–	–	2.3	0.5

quantitation. CE sodium adducts were used for the quantitation in case of UHPSFC/MS. CE cannot be quantified using HILIC/MS platforms due to massive ion-source fragmentation leading to the fragment ion at *m/z* 369.3 ([cholesterol + H–H_2O]$^+$ ion) without any precursor ion information needed for the quantitation of CE species. Cer provided [M+H]$^+$, [M+Na]$^+$, and [M + H–H_2O]$^+$ ions, with the latter ion used for the quantitation. Ammonium adducts were used for the quantitation of TG lipid class, but sodium adducts were present as well. Similarly, for DG lipid class, the same adducts were present as in the case of TG, with additional [M + H–H_2O]$^+$ ions showing a higher response, and, therefore, [M + H–H_2O]$^+$ ions were used for the DG quantitation. MG lipid class shows a higher response for [M+Na]$^+$ adduct than for [M + H–H_2O]$^+$ and [M + NH_4]$^+$ ions, and, consequently, the sodium adducts were used for the quantitation of MG.

Generally, ratios between present adducts are higher for measurements by HILIC/MS platforms than for UHPSFC/MS platforms (Table 1). This can be explained by different composition of mobile phase that influences the ionization. From the MS point of view, the Xevo mass spectrometer shows higher responses of adducts than the Synapt mass spectrometer, independent of the chromatographic mode used.

3.3. Lipid species determined in human plasma samples by the four analytical platforms

Numbers of lipid species determined in human plasma samples by individual platforms are shown in Table 2, and lipid species quantified by the individual analytical platforms are listed in Table S-3 in ESM. Generally, a higher number of lipid species was determined by UHPSFC/MS in comparison to HILIC/MS, which is mainly attributed to the impossibility of DG, MG, and CE quantitation by HILIC/MS. When different mass spectrometers were compared, a higher number of lipid species could be detected with the Xevo mass spectrometer than with the Synapt mass spectrometer in both chromatographic modes, probably because of a better sensitivity of the instrument. To compare measurements of the four analytical platforms, only lipid species determined by all platforms were used for the further evaluation.

3.4. Lipid profiles obtained by the four analytical platforms

The relative abundances of individual classes for NIST plasma sample (Fig. 1) provide comparable results for all analytical platforms. For HILIC/MS, TG lipid class shows the highest relative response (above 50%), followed by PC (around 40%), LPC, SM, and Cer. UHPSFC/MS platforms show a similar trend with the highest response also for TG (above 54%), followed by PC (around 30%), and CE, LPC, SM, DG, Cer, and MG. The percentages mentioned were normalized to the total signal of individual platforms. The comparability of lipid profiles for all configurations and all lipid classes (PC, SM, LPC, Cer, TG, DG, MG, and CE) is shown in Fig. S-2, including NIST plasma measurements (intensities) acquired at the beginning, in the middle, and at the end of the sequence (mean value of intensities). Relative intensities are expressed by percentage and related to the lipid species with the highest response (100%) (Fig. S-2). All lipid profiles obtained by the four analytical platforms exhibit high visual similarities.

3.5. Quality control

An important task during the measurements of clinical samples is a quality control (QC) system using QC samples to assess the data comparability and integrity. QC samples were regularly injected during the sequence after every 40 samples. Concentrations of lipids in QC samples should be the same over the whole sequence, as illustrated by the clustering of QC samples in the PCA plot prepared for UHPSFC-Synapt platform (Fig. S-3). Similar plots were obtained for other platforms as well (data not shown).

The comparison of the four analytical platforms were also made according to the reproducibility of the obtained lipid concentrations expressed as the relative standard deviation (RSD) of all QC samples (Table S-3). The majority of common lipid species for all analytical platforms showed RSD below 20%, indicating a good reproducibility of lipid concentration measurements during the entire sequence. The RSD between 20 and 40% is observed for some lipid species of lower abundancy (e.g., TG 47:0, Cer 34:1, PC 32:2, PC 40:4, SM 33:1, and LPC 16:1) mainly for HILIC/MS platforms, which generally provides slightly lower concentration reproducibility than UHPSFC/MS platforms likely caused by higher signal background. Some lipid classes, such as CE, DG, and MG quantified by UHPSFC/MS platforms, showed good concentration reproducibility (<25%) except for some lipid species encountered in trace concentrations, indicating that lower reproducibility may be associated with the concentrations near the limit of quantitation.

During the long run sequences, a signal drop due to a gradual contamination of the mass spectrometer is observed. To compare the four platforms based on the signal stability, we used a dependence of signal drop (expressed by percentage; first sample as 100%) of exogenous lipids (added before the extraction; included in our IS mix) on the run sequence number (Fig. S-4A-G). The signal drop is observed for all platforms. The decrease of signal during the run sequence from the injection of the first sample to the injection of the last sample is about 79% for UHPSFC-Xevo, 49% for UHPSFC-Synapt, and 57% for HILIC-Synapt, but reaches 90% in the case of HILIC-Xevo. The signal usually drops faster at the beginning of the sequence and the decrease then gradually slows down, with a higher decrease observed for the Xevo mass spectrometer compared to the Synapt mass spectrometer. Regarding the different chromatographic modes, higher signal decrease is observed for HILIC/MS platforms than for UHPSFC/MS platforms, which proves that UHPSFC contributes to the lower contamination of mass spectrometers, which could be attributed to the flow splitting in case of UHPSFC. The intensity decreases are quite well compensated using IS for the quantitation. The intensity of lipid species is divided by the intensity of the corresponding lipid class IS multiplied by the known concentration of IS (Fig. S–4H–N).

3.6. Quantitation errors for individual platforms

At least 2 IS per lipid class are included in the IS-Mix (except for CE), which is added to the human plasma samples before the extraction. This allows the calculation of the quantitation error expressed as the percentage using following formula: 100*concentration of IS (not used for quantitation) obtained from measurements (experimental value) divided by theoretical concentration of IS (known from IS Mix) using all 268 samples (average value). Values of quantitation errors for SM 30:1,

Table 2
Numbers of lipid species determined in human plasma samples by four platforms. CE – cholesteryl esters; MG – monoacylglycerols; DG – diacylglycerols, TG – triacylglycerols; Cer – ceramides; PC – glycerophosphocholines; LPC – glycerolysophosphocholines; and SM – sphingomyelins.

Platform		TG	DG	MG	Cer	PC	LPC	SM	CE	Total number of lipids	Number of common lipids
1	HILIC-XEVO	56	–	–	9	32	7	21	–	125	73
2	HILIC-SYNAPT	32	–	–	6	30	6	17	–	91	73
3	UHPSFC-XEVO	68	22	3	9	39	7	20	8	176	73
4	UHPSFC-SYNAPT	56	20	3	9	32	7	17	7	151	73

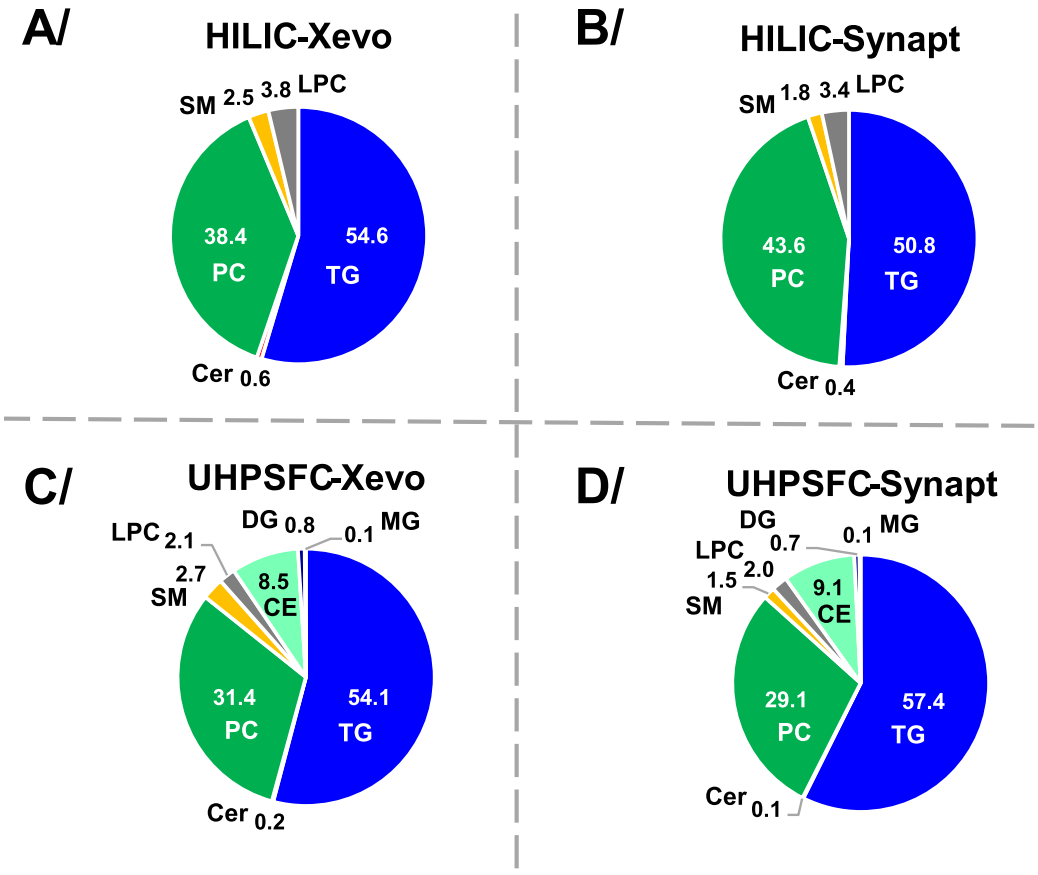

Fig. 1. Relative intensity responses (%) of lipid classes illustrated with NIST plasma measurements for: (A) HILIC-Xevo, (B) HILIC-Synapt, (C) UHPSFC-Xevo, and (D) UHPSFC-Synapt analytical platforms. TG – triacylglycerols, DG – diacylglycerols, MG – monoacylglycerols, CE – cholesteryl esters, Cer – ceramides, PC – phosphatidylcholines, LPC – lysophosphatidylcholines, and SM – sphingomyelins.

LPC 17:0, and PC 28:0 are within ±15% for all platforms except for PC 28:0 for HILIC-Xevo, where the error is −24.3%. In the case of TG 57:3 IS, UHPSFC/MS platforms provide better quantitation error (<20%) than HILIC/MS platforms. DG and MG quantified by UHPSFC/MS platforms have quantitation error within ±15% except for DG 36:5 d5 for UHPSFC-Xevo (18.4%). For Cer 35:1, the quantitation error is beyond ±15% limits, but RSD of quantitation errors of all IS obtained for all platforms is less than 16%, providing a proof of good reproducibility for all platforms. All results of calculation are shown as bar plots (Fig. 2). The quantitation approach was cross examined using an exogenous IS for the quantitation of deuterated ones with the same outcomes (Fig. S–5H). The different visualization of the closeness of theoretical concentrations of IS to the practical values are shown in Fig. S-4 and Fig. S-5A-G.

The analysis of the high quantitation error of ceramide IS indicates that the signal response does not correspond to the concentrations in the IS-Mix. Cer 35:1 was purchased as a powder and stock solution of 2 mg/mL was prepared, but deuterated ceramide IS (Cer 36:1 d7) at the concentration of 1 mg/mL was purchased. Observed discrepancies in the signal response can be caused by the decomposition of the stock solutions, a mismatch of the delivered concentration, or a mismatch in the isotopic distribution of the deuterated IS.

3.7. Comparison of lipid concentrations among data sets

Concentrations of common lipid species determined in 268 human plasma samples and NIST plasma sample are summarized in Table S-4. The differences of lipid concentrations determined by the four analytical platforms were expressed using the RSD (%). The comparison of results obtained for HILIC chromatographic mode using two mass spectrometers shows high agreement for almost all lipid species across a range of concentrations. The RSD is usually below 20% or between 20 and 30%, with the exception of few lipid species, such as TG 48:0, PC O-38:5/P-38:4, PC 36:1, PC 40:7, PC 40:5, or PC 40:4, for which the RSD is above 40% for all samples (Table S-5). A similar trend is seen for UHPSFC hyphenated to the two mass spectrometers. The comparison shows even higher similarities of the concentrations obtained by using the mass spectrometers other than the HILIC/MS platforms except for the lipid species TG 46:0, CE 22:6, DG 30:0, DG 38:2, or MG 16:0, for which the highest concentration discrepancies were observed (RSD is between 30 and 40% or higher than 40% for almost all samples; Table S-6). The concentrations obtained for different chromatographic modes (HILIC and UHPSFC) connected to the same mass spectrometer were compared as well. Concentrations obtained from measurements by HILIC-Xevo and UHPSFC-Xevo platform shows minor concentration variations for almost all lipid concentrations except for the lipid species TG 51:5, TG 56:7, PC 40:7, and LPC 20:4, for which the RSD is higher than 40% (Table S-7). Higher concentration variations were observed for the Synapt mass spectrometer coupled to the two different chromatographic modes (Table S-8). The RSD higher than 40% is observed for the same lipids as for Xevo mass spectrometer and for the lipid species PC 36:5, Cer 32:3 (OH), TG 46:0, TG 47:0, and TG 49:2.

The overall differences in lipidome quantitation are more influenced by different chromatographic modes than different mass spectrometers for TG, Cer, and LPC lipid classes, but, generally, the mean RSD for all lipid species in all samples is below 30% (Table 3).

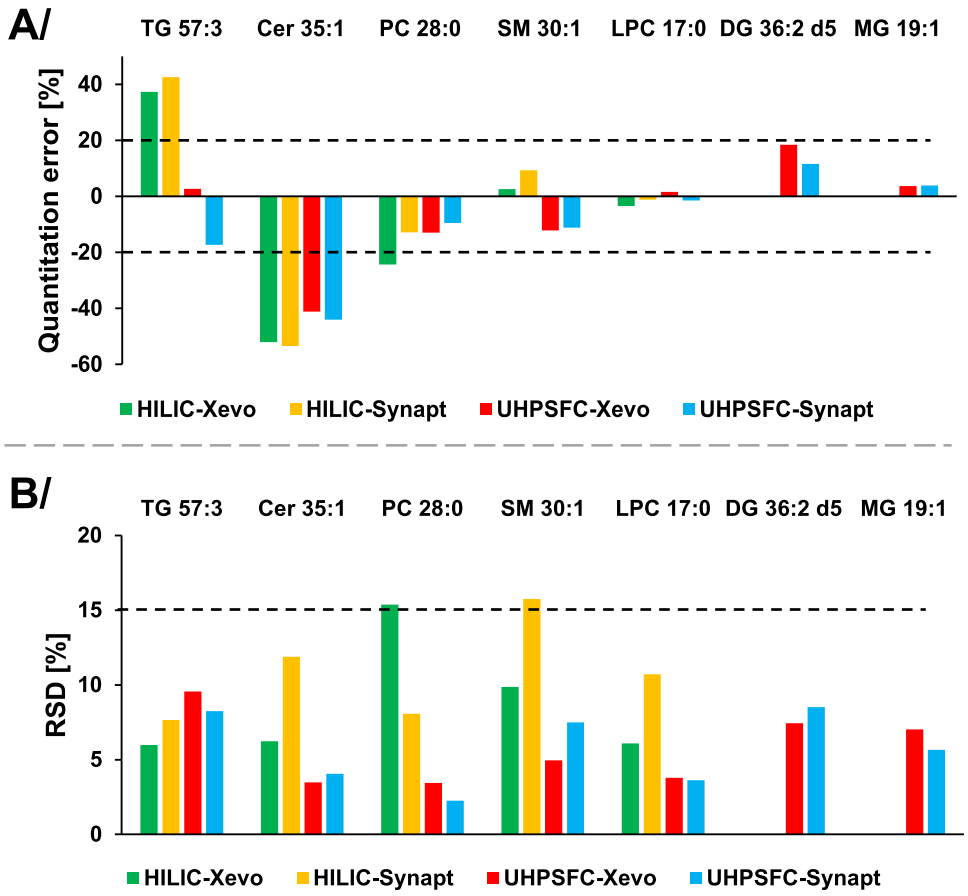

Fig. 2. Relative quantitation errors (A) and RSD of the quantitation error (B) for four analytical platforms. TG – triacylglycerols, DG – diacylglycerols, MG – monoacylglycerols, Cer – ceramides, PC – phosphatidylcholines, SM – sphingomyelins, and LPC – lysophosphatidylcholines.

Table 3
Average of RSD for all lipid species in all samples (sum) between HILIC-MS (A), UHPSFC-MS (B), Xevo (C), and Synapt (D) platforms. TG – triacylglycerols, Cer – ceramides, PC – phosphatidylcholines, SM – sphingomyelins, and LPC – lysophophatidylcholines; SD – standard deviation.

	Chromatograhic mode	Mass spectrometer	TG		Cer		PC		SM		LPC	
			RSD [%]	SD	RSD [%]	SD	RSD [%]	SD	RSD [%]	SD	RSD [%]	SD
A	HILIC	Xevo vs. Synapt	**17**	9	**10**	5	**27**	13	**16**	3	**14**	6
B	UHPSFC	Xevo vs. Synapt	**20**	19	**14**	4	**20**	11	**9**	4	**12**	5
C	HILIC vs. UHPSFC	Xevo	**18**	13	**12**	9	**14**	11	**12**	3	**27**	29
D	HILIC vs. UHPSFC	Synapt	**29**	20	**22**	9	**16**	10	**8**	3	**28**	30

Inter-dependencies of the four platforms were also demonstrated by correlation plots. The correlation plots were created using the decimal logarithms of concentrations (pmol/mL) of lipids obtained from HILIC/MS or UHPSFC/MS measurements in two types of human plasma samples from different sources, i.e. NIST plasma reference material (Fig. S-6) and our QC pooled sample (Fig. S-7). All models show similarities, in particular for polar lipid classes, such as SM and LPC. Slightly lower variations are observed for UHPSFC/MS (Fig. S–6B) in comparison to HILIC/MS (Fig. S–6A) demonstrating (together with RSD calculations) is the utility of the UHPSFC mode in the lipidomic quantitation. Correlations between the same mass spectrometers connected to different chromatographic mode reflect the same results as RSD calculations, thus better correlations for the Xevo mass spectrometer (Fig. S–6C) than for the Synapt mass spectrometer (Fig. S–6D). The same results have been observed for correlation plots created from concentrations in QC pooled samples (Fig. S-7).

To visualize the consistency of lipid concentrations across all platforms, box plots were prepared based on molar concentrations (nmol/mL) of lipid species determined in human plasma samples of healthy volunteers and renal cell carcinoma patients. Lipids with high (Fig. S-8), medium (Fig. S-9), and low abundance (Fig. S-10) in human plasma within one lipid class were selected. These examples demonstrate a good comparability for the lipid species of medium abundance. The concentration differences expressed as a percentage for healthy volunteers and renal cell carcinoma patients are shown in Table S-9. In case of different mass spectrometers, the Xevo mass spectrometer provides slightly higher concentrations in comparison to the Synapt mass spectrometer in almost all cases of quantified lipid species for the UHPSFC chromatographic mode. The opposite is observed for the highly abundant lipid species, such as TG 52:2, TG 52:3, PC 34:2, PC 34:1, SM 34:1, and LPC 16:0, for which the Synapt instrument provides higher concentration values. A similar trend is observed for measurements in HILIC chromatographic mode. The comparison of HILIC and UHPSFC chromatographic modes connected to the same mass spectrometer shows that HILIC/MS platforms provide higher concentration values for almost all lipid species than UHPSFC/MS platforms except for some lipids of low

abundance.

3.8. Statistical comparison of the four platforms in renal cell carcinoma study

The influence of the analytical platform on the distinguishing two groups of subjects was investigated. Lipid concentrations in plasma samples from renal cell carcinoma patients (N = 173) and healthy controls (N = 95) were compared for the different platforms. PCA and OPLS-DA were performed for the statistical evaluation. First, the data were pre-processed using Pareto scaling and logarithmic transformation. Fig. 3 shows the OPLS-DA plots created from molar concentrations (nmol/mL) of lipids of healthy volunteers (blue dots) and renal cell carcinoma patients (red dots) measured by all platforms demonstrating a high degree of similarity. The comparison of these models was done by comparing the sensitivity, specificity, and accuracy values (Table 4). The sensitivity is the true positive rate to correctly predict that samples are obtained from cancer patients. The specificity is the true negative rate to correctly predict that samples are obtained from the healthy control group and the accuracy describes the overall prediction performance. Excellent correlations of results were obtained for all platforms (Table 3), with specificity, sensitivity, and accuracy being approximately 72%, 87%, and 82%, respectively. In order to visualize the most dysregulated lipids (for all analytical platforms) influencing the separation of samples into two groups, the fold change was calculated and a heatmap was constructed (Table S-10). The heatmap illustrates up-regulated (reddish colors) and down-regulated (blueish colors) lipid species determined in human plasma samples of the renal cell carcinoma study. Calculated fold changes also show high similarities between the four platforms with regard to discovered regulated lipid species obtained by individual platforms used in this work. This fact proves that small variations in lipid concentrations obtained by the four platforms do not influence the distinguishing of sample groups.

Table 4
Specificity, sensitivity, and accuracy of statistical models obtained from measurements of healthy volunteers and renal cell carcinoma patients by 4 analytical platforms.

Platform	Specificity [%]	Sensitivity [%]	Accuracy [%]
HILIC-Xevo	72.6	88.4	82.8
HILIC-Synapt	74.5	86.7	82.5
UHPSFC-Xevo	71.6	86.7	81.3
UHPSFC-Synapt	69.5	89.6	82.5

Clinical studies with human samples often exhibit some outliers due to various reasons, including biological variance, lifestyle of patients, or occult diseases. PCA1 score plot for PC 36:2 (Fig. S-11) illustrates that the same outliers are observed in the renal cell carcinoma study indicating the robustness of these analytical platforms that can reproducible detect outliers regardless of the method and instrument configuration, an important finding for multi-laboratory studies.

3.9. Normalization of lipid concentrations among different platforms

The normalization may be a useful tool to diminish platform-specific differences in lipid concentrations [23]. The normalization was performed for each analytical platform and all samples. The lipid concentration of a given sample is divided by the mean lipid concentration of NIST plasma samples and multiplied by the lipid concentration in NIST plasma (average value of the four platforms). Fig. 4 shows PCA plots for the renal cell carcinoma sample set employing the four platforms, with Fig. 4A and **B** (QC samples highlighted) illustrating the lipid concentration differences before the normalization and Fig. 4C and D (QC

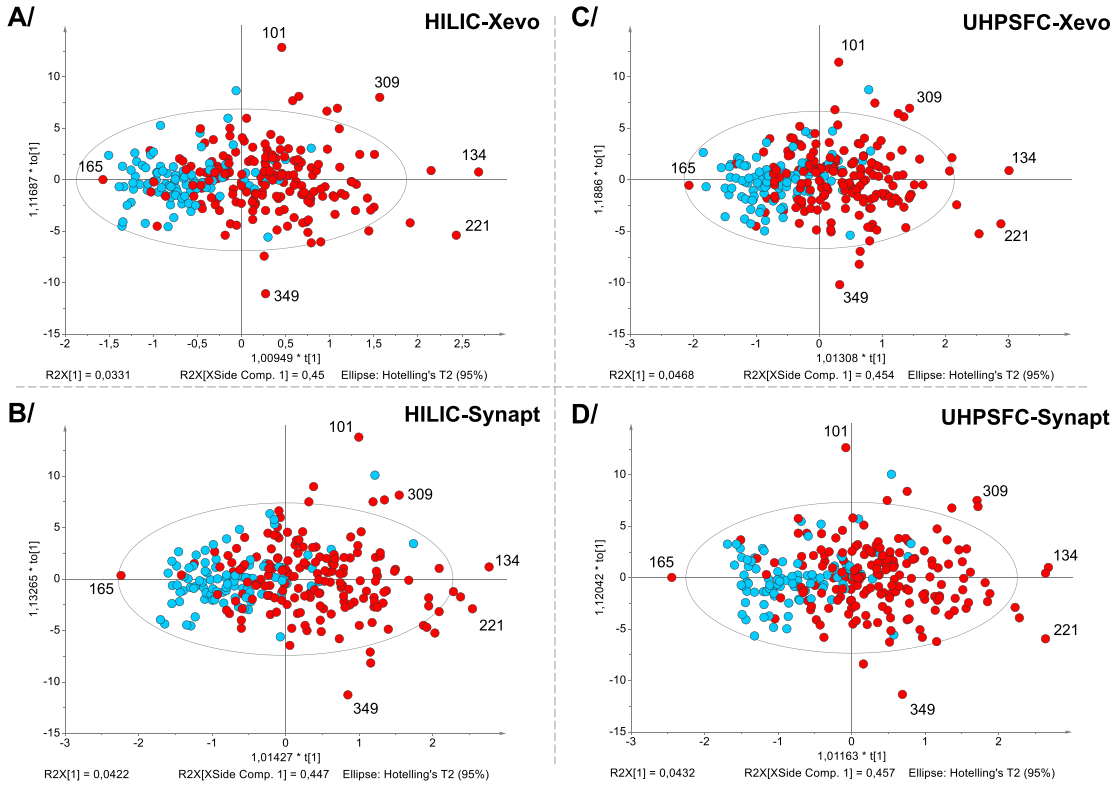

Fig. 3. OPLS-DA score plots constructed from molar concentrations of lipids determined in healthy volunteers (blue) and renal cell carcinoma patients (red) by: (A) HILIC-Xevo, (B) HILIC-Synapt, (C) UHPSFC-Xevo, and (D) UHPSFC-Synapt. Selected outliers are annotated by the sample number. The same numbers of healthy volunteers (95), renal cell carcinoma patients (173), and same number of variables (73 common lipid species) were used for each platform. (For interpretation of the references to colour in this figure legend, the reader is referred to the web version of this article.)

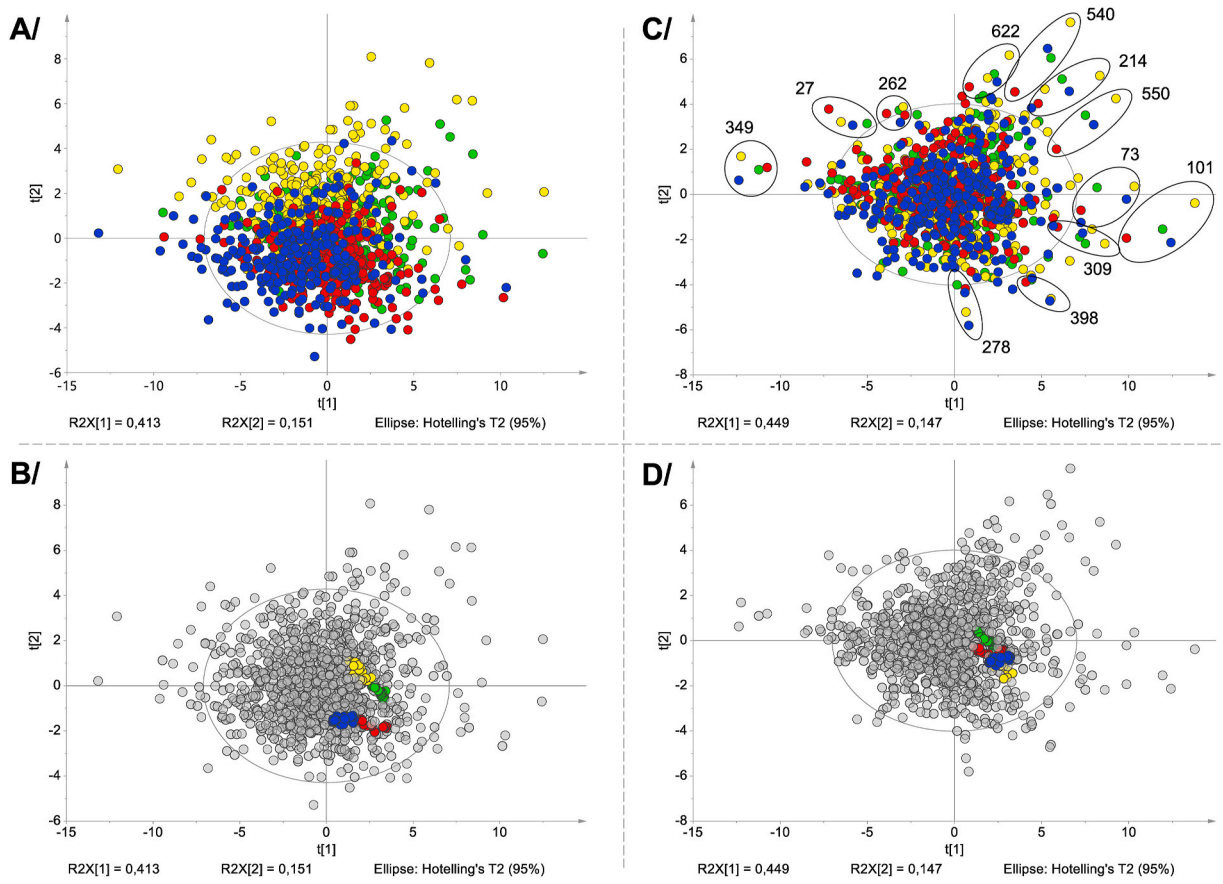

Fig. 4. PCA score plot of HILIC-Xevo (green), HILIC-Synapt (yellow), UHPSFC-Xevo (red), and UHPSFC-Synapt (blue) platforms prepared from the data before normalization (A) and after normalization (C) with highlighting of all samples and highlighting only QC samples for non-normalized (B) and normalized data (D). Selected outliers are annotated by the sample number. The same numbers of healthy volunteers (95), renal cell carcinoma patients (173), and same number of variables (73 common lipid species) were used for each platform. (For interpretation of the references to colour in this figure legend, the reader is referred to the web version of this article.)

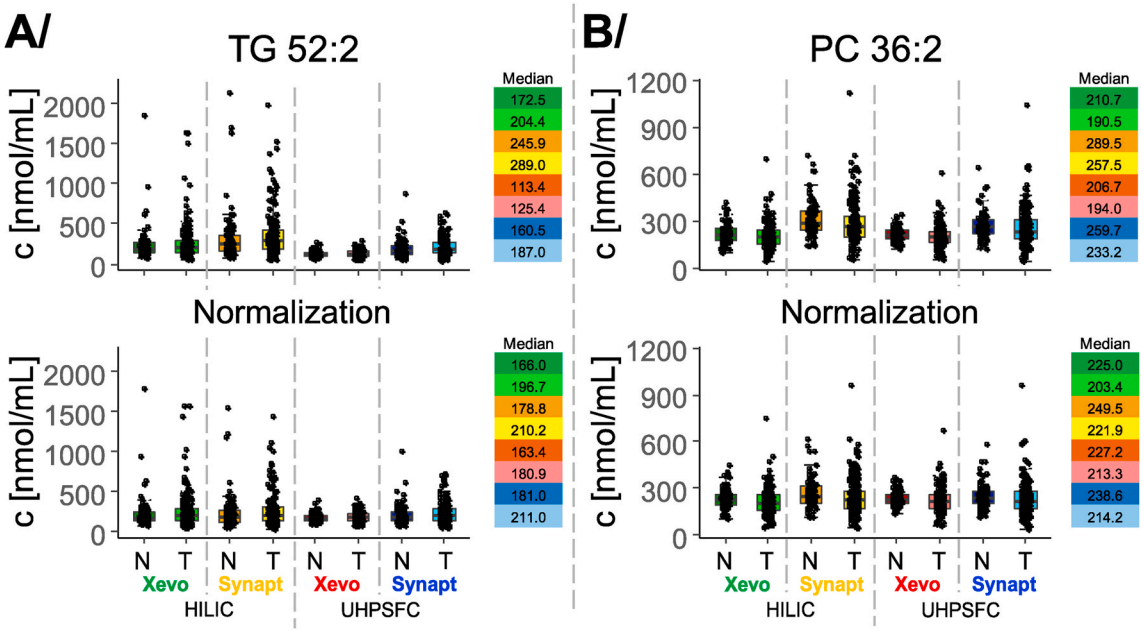

Fig. 5. Box plots before and after the normalization for selected representatives of non-polar and polar lipid classes: (A) TG 52:2 and (B) PC 36:2. TG – triacylglycerols, PC – phosphatidylcholines.

samples highlighted) demonstrating the lipid concentration differences after the normalization. Better clustering of QC samples after the normalization highlights the effect of the normalization on the statistical models (Fig. 4B and D).

For the detailed description of normalization, we have used these normalized data to create correlation plots and box plots. Normalized data provide significantly better correlation results (Fig. S-12) among individual platforms, which is illustrated also in box plots with medians (Fig. 5), but without changing of observed outcomes of statistical results (Table S–10B). The distinction between the two groups from normalized data shows the same statistical models with the same specificity, selectivity, and accuracy. This indicates that the normalization is a useful tool to reduce biases in intra- and inter-laboratory studies without losing the quality of statistical models, which is quite important for multi-laboratory clinical trials.

4. Conclusions

Small differences in lipid concentrations were observed even during measurements with the settings similar as much as possible. These concentration discrepancies can be even higher, if results are obtained from different laboratories using different extraction protocols, and different instrumentation. However, small differences in the present data sets can be further reduced using the normalization with parallel measurements of lipid concentrations in the reference sample of NIST plasma or other reference material used as QC samples. The key conclusion of the present study is that the ultimate results of renal cell carcinoma diagnostic study are to a high degree comparable among all platforms both for non-normalized and normalized data, which proves a high robustness of the methods developed for the quantitation of lipids in biological samples.

Credit author statement

Michaela Chocholoušková; : Methodology, Formal analysis, Investigation, Writing – original draft, Visualization; Denise Wolrab: Investigation, Writing – review & editing; Robert Jirásko: Methodology, Writing – review & editing; Hana Študentová; : blood collection, Resources, Writing – review & editing; Bohuslav Melichar: Resources, Writing – review & editing; Michal Holčapek: Resources, Project administration, Supervision, writing-review and editing.

Funding information

This work was supported by the grant project No. 18-12204S funded by the Czech Science Foundation.

Compliance with ethical standards

The study was approved by the ethical committee, and all healthy volunteers signed informed consent.

Declaration of competing interest

The authors declare that they have no known competing financial interests or personal relationships that could have appeared to influence the work reported in this paper.

Appendix A. Supplementary data

Supplementary data to this article can be found online at https://doi.org/10.1016/j.talanta.2021.122367.

References

[1] M.R. Wenk, The emerging field of lipidomics, Nature Reviews 4 (2005) 594–610.
[2] G. Liebisch, R. Ahrends, A. Makoto, A. Masanori, J.A. Bowden, C.S. Ejsing, W. J. Griffiths, M. Holčapek, H. Köfeler, T.W. Mitchell, M.R. Wenk, K. Ekroos, Lipidomics need more standardization, Nat. Metab. 1 (2019) 745–747.
[3] K. Ekroos, Lipidomics perspective: from molecular lipidomics to validated clinical diagnostics. Lipidomics: Technologies and Applications, Wiley-VCH Verlag & Co. KGaA, Weinheim, Germany, 2012, pp. 1–19.
[4] A. Schevchenko, K. Simons, Lipidomics: coming to grips with lipid diversity, Nat. Rev. Mol. Cell Biol. 11 (2010) 593–598.
[5] M.R. Wenk, Lipidomics: new tools and applications, Cell 143 (2010) 888–895.
[6] M. Holčapek, G. Liebisch, K. Ekroos, Lipidomic analysis, Anal. Chem. 90 (2018) 4249–4257.
[7] The Lipid Maps, 2003-2021. https://www.lipidmaps.org/resources/tutorials/lipid_tutorial.php#D. (Accessed 17 November 2020).
[8] E. Fahy, S. Subramaniam, H.A. Brown, C.K. Glass, A.H. Merrill Jr., R.C. Murphy, C. R.H. Raetz, D.W. Rusell, Y. Seyama, W. Shaw, T. Shimizu, F. Spener, G. van Meer, M.S. VanNieuwenhze, S.H. White, J.L. Witztum, E.A. Dennis, A comprehensive classification system for lipids, J. Lipid Res. 46 (2005) 839–862.
[9] W.W. Christie, High-performance Liquid Chromatography and Lipids: A Practical Guide, Pergamon Press, Oxford, 1987.
[10] T. Čajka, O. Fiehn, Comprehensive analysis of lipids in biological systems by liquid chromatography-mass spectrometry, TrAC Trends Anal. Chem. (Reference Ed.) 61 (2014) 192–206.
[11] B. Burla, M. Arita, M. Arita, A.K. Bendt, A. Cazenave-Gassiot, E.A. Dennis, K. Ekroos, X. Han, K. Ikeda, G. Liebisch, M.K. Lin, T. Ping Loh, P.J. Meikle, M. Orešič, O. Quehenberger, A. Shevchenko F. Torta, M.J.O. Wakelam, C. E. Wheelock, M.R. Wenk, MS-based lipidomics of human blood plasma: a community-initiated position paper to develop accepted quidelines, J. Lipid Res. 59 (2018) 2001–2017.
[12] T. Čajka, O. Fiehn, Toward merging untargeted and targeted methods in mass spectrometry-based metabolomics and lipidomics, Anal. Chem. 88 (2016) 524–545.
[13] D. Wolrab, R. Jirásko, M. Chocholoušková, O. Peterka, M. Holčapek, Oncolipidomics: mass spectrometric quantitation of lipids in cabcer research, TrAC Trends Anal. Chem. (Reference Ed.) 120 (2019) 115480.
[14] M. Wang, C. Wang, X. Han, Selection of internal standards for accurate quantification of complex lipid species in biological extracts by electrospray ionization mass spectrometry - what, how and why? Mass Spectrom. Rev. 36 (2017) 693–714.
[15] E. Cífková, M. Lísa, R. Hrstka, D. Vrána, J. Gatěk, B. Melichar, M. Holčapek, Correlation of lipidomic composition of cell lines and tissues of breast cancer patients using hydrophilic interaction chromatography/electrospray ionization mass spectrometry and multivariate data analysis, Rapid Commun. Mass Spectrom. 31 (2017) 253–263.
[16] M. Lísa, M. Holčapek, High-throughput and comprehensive lipidomic analysis using ultrahigh-performance supercritical fluid chromatography-mass spectrometry, Anal. Chem. 87 (2015) 7187–7195.
[17] J.H. Gross, Mass Spectrometry: a Textbook, second ed., Springer, New York, 2011.
[18] B. Simons, D. Kauhanen, T. Sylvänne, K. Tarasov, E. Duchoslav, K. Ekroos, Shotgun lipidomics by sequential precursor ion fragmentation on a hybrid quadrupole time of flight mass spectrometer, Metabolites 2 (2012) 195–213.
[19] T. Čajka, J.T. Smilowitz, O. Fiehn, Validating quantitative untargeted lipidomics across nine liquid chromatography-high-resolution mass spectrometry platforms, Anal. Chem. 89 (2017) 12360–12368.
[20] J.A. Bowden, A. Heckert, C.Z. Ulmer, C.M. Jones, J.P. Koelmel, L. Abdullah, L. Ahonen, Y. Alnouti, A.M. Armando, J.M. Asara, T. Bamba, J.R. Barr, J. Bergquist, C.H. Borchers, J. Brandsma, S.B. Breitkopf, T. Čajka, A. Cazenave-Gassiot, A. Checa, M.A. Cinel, R.A. Colas, S. Cremers, E.A. Dennis, J.E. Evans, A. Fauland, O. Fiehn, M.S. Gardner, T.J. Garrett, K.H. Gotlinger, J. Han, Y. Huang, A. Huipeng Neo, T. Hyötyläinen, Y. Izumi, H. Jiang, H. Jiang, J. Jiang, M. Kachman, R. Kiyonami, K. Klavins, C. Klose, H.C. Köfeler, J. Kolmert, T. Koal, G. Koster, Z. Kuklenyik, I.J. Kurland, M. Leadley, K. Lin, K. Rao Maddipati, D. McDougall, P. J. Meikle, N.A. Mellett, C. Monnin, M.A. Moseley, R. Nandakumar, M. Orešič, R. Patterson, D. Peake, J.S. Pierce, M. Post, A.D. Postle, R. Pugh, Y. Qiu, O. Quehenberger, P. Ramrup, J. Rees, B. Rembiesa, D. Reynaud, M.R. Roth, S. Sales, K. Schuhmann, M. Laniado Schwartzman, C.N. Serhan, A. Shevchenko, S. E. Somerville, L.St John-Williams, M.A. Surma, H. Takeda, R. Thakare, J. Will Thompson, F. Torta, A. Triebl, M. Trötzmüller, S.J. Kumari Ubhayasekera, D. Vuckovic, J.M. Weir, R. Welti, M.R. Wenk, C.E. Wheelock, L. Yao, MYuan, X. Heather Zhao, S. Zhou, Harmonizing lipidomics: NIST interlaboratory comparison exercise for lipidomics using SRM 1950 Metabolites in Frozen Human plasma, J. Lipid Res. 58 (2017) 2275–2288.
[21] D. Wolrab, M. Chocholoušková, R. Jirásko, O. Peterka, M. Holčapek, Validation of lipidomic analysis of human plasma and serum by supercritical fluid chromatography-mass spectrometry and hydrophilic interaction liquid chromatography-mass spectrometry, Anal. Bioanal. Chem. 412 (2020) 2375–2388.
[22] R. Jirásko, M. Holčapek, M. Khalikova, D. Vrána, V. Študent, Z. Prouzová, B. Melichar, MALDI Orbitrap mass spectrometry profiling of dysregulated sulfoglycosphingolipids in renal cell carcinoma tissues, J. Amer. Mass Spectrom. Soc. 28 (2017) 1562–1574.
[23] A. Triebl, B. Burla, J. Selvalatchmanam, J. Oh, S. Hwee Tan, M.Y. Chan, N. A. Mellet, P.J. Meikle, F. Torta, M.R. Wenk, Shared reference materials harmonize lipidomics across MS-based detection platforms and laboratories, J. Lipid Res. 61 (2019) 105–115.